

Effect of Novel Ribs in Parallel Channel Low Temperature PEMFC Performance[#]

Alisha Daimari^{1,2}, Atul Sharma¹, Shyamprasad Karagadde¹, Shyamkumar P I²

1 Department of Mechanical Engineering, Indian Institute of Technology Bombay, Mumbai 400076, Maharashtra, India

2 Cummins Technologies India Pvt. Limited, Pune 411038, Maharashtra, India

(Corresponding Author: alisha.daimari@cummins.com)

ABSTRACT

Flow channel or flow field designs have a significant impact on the performance of a Proton Exchange Membrane Fuel Cell (PEMFC). These channels are essential for distributing reactant gases, eliminating byproducts like water, and managing heat within the cell. Enhancing the flow field design can improve the efficiency, power output, and overall lifespan of PEMFCs. A three-dimensional multiphysics, two-phase PEMFC model with novel ribs in the form of asymmetrical airfoil in a parallel flow channel has been investigated in the present study. The ribs are placed along the length of the channel equidistantly. With the operating parameters kept constant, effect of different types of ribs on the overall performance of the fuel cell is reported and compared with the Baseline case where no ribs are present. The present model comprises of a single unit PEMFC modelled in the commercial software package ANSYS Fluent version 2023R2. A comparative study on the effects of different ribs shapes like rectangular, circular and asymmetrical airfoil on the overall PEMFC performance is presented. The obstruction in the flow channel is observed to improve the polarization curve, i.e., current vs. voltage (I-V) curve as well as current vs. power (I-P) curve, in other words, the fuel cell performance. Pressure drop is found higher for parallel flow channel with rectangular ribs than baseline without ribs. Thus, this study examines how a different flow channel design with ribs affects PEMFC performance metrics, offering insights into how changes in flow field configuration can propel advancements in fuel cell technology.

Keywords: PEM Fuel Cell, Computational Fluid Dynamics, Performance, Airfoil, Operating parameter.

NONMENCLATURE

Abbreviations

CL	Catalyst Layer
GDL	Gas Diffusion Layer

PEMFC	Proton Exchange Membrane Fuel Cell
<i>Symbols</i>	
c_p	Specific heat at constant pressure (J/kg K)
C	molar concentration (mol/m ³)
D	coefficient of diffusion (m ² /s)
E	Nernst potential (V)
F	Faraday constant (96487 C/mol)
G ₀	Gibbs free energy per mole (J/mol)
h	molar formation enthalpy (J/mol)
I	exchange current density (A/m ²)
j	volumetric exchange current density (A/ m ³)
k	thermal conductivity (W/mK)
K	absolute permeability (m ²)
M	molar mass (kg mol)
α	transfer coefficient
β	protonic conduction coefficient
γ	concentration dependence
ϵ	porosity
η	over potential (V)
λ	water content in the membrane
σ	membrane conductivity (S/m)
ϕ	electric potential (V)

1. INTRODUCTION

Fuel cell modelling has been an important milestone in the advancement of Proton Exchange Membrane Fuel Cell (PEMFC) technology by facilitating better insights of electrochemical reactions, thermodynamics, and fluid dynamics. Recently many models utilizing computational fluid dynamics (CFD) have been established to simulate complex multi-phase, multi-component, and multi-dimensional interactions in irregular geometries, supporting research in areas like flow field design and water and thermal management [1].

Inclusion of flow directing feature in a flow channel has been studied and found to influence the performance by impacting mass transport, pressure drop, and water

[#] This is a paper for the 16th International Conference on Applied Energy (ICAE2024), Sep. 1-5, 2024, Niigata, Japan.

management. According to the works of Tiss et al. [2], for the analysis of fuel cell polarization and power density, partial blocks in the flow channels tilted at 4.9° show better performance than those at 6.6° and 8.2°, as observed in the polarization and power curves. Li and Sabir [3] summarize their research examining how the shape of reactant flow paths such as parallel, serpentine, and inter-digitated through a PEM stack impact several parameters, including reaction rates, the distribution of reactants within a PEM stack, water removal capability, and pressure drop. According to Scholta et al.'s [4] numerical study, smaller dimensions of gas channels are favored at high current densities, while larger ones perform better at low current densities. Wang et al. [5] conducted a numerical study that revealed at high operating voltages and low current densities, oxygen can adequately reach the reaction region, rendering the impact of channel design on PEMFC performance negligible. Conversely, at low operating voltages and high current densities, channel design becomes crucial for PEMFC performance, with smaller cross-sectional areas improving water removal and thus performance. Sun et al. [6] found that the size ratio of a PEMFC with a trapezoidal cross-sectional shape significantly impacts the flow crossover. In a comparative study by Ahmed and Sung [7] between rectangular and trapezoidal channel shapes showed that rectangular channels produced more power, but trapezoidal channels resulted in more uniform reactant and current density distribution, leading to lower overpotential. Additionally, it was observed that increasing shoulder width decreased ohmic loss but increased concentration loss. In a similar study, Ghanbarian and Kermani [8] reported the performance improvement when partial blockage in different shapes like square, semicircle and trapezoid are introduced in the parallel flow channels. In another study, Wang et al. [9] utilized an optimization process that combined a simplified conjugate-gradient method with a three-dimensional, two-phase, non-isothermal model to optimize the flow field design of a serpentine PEMFC featuring five channels with varied heights. Heidary and Kermani [10] explored the heat transfer dynamics in wavy flow channels. Their research demonstrated that heat transfer in wavy channels could improve by up to 100%, depending on factors such as wave number, wave amplitude, and Reynolds number. Shimpalee and Van Zee [11] numerically explored the impact of rib size on PEMFC performance, finding that narrower channels improved heat conduction through the bipolar plate, resulting in a lower, more consistent temperature, higher membrane water content, and

better polarization curves. Hsieh and Chu's [12] experimental findings indicated that the optimal channel size, when balancing pressure drop and power output, differed from the size determined when only considering power output.

The performance of PEM fuel cells for a constant cell active area can be summarized to be affected by the design changes in the flow channels such as:

Sequential or abrupt change along the length of flow channels can have steady and progressive or sudden effects respectively in the local current density, influence of shape and size of the cross-sectional area of overall flow channel in the likes of rectangle, square, trapezoid, triangle, semicircle etc., and symmetric or asymmetric patterns of ribs along the length of channel with different shapes and dimensions are reported to be influential. Additionally, the angle at which the flow direction meets the temperature gradient can be adjusted by employing some partial ribs or blocks.

A three-dimensional single unit PEM Fuel Cell model comprising the membrane, Catalyst Layers (CL), Gas Diffusion Layers (GDL), flow channels and current collectors is investigated in the present study. The flow channels are parallel in nature with co-flow. To investigate the effect of partial ribs or blocks on the overall performance of PEM fuel cells, a novel rib in the shape of asymmetrical airfoil is studied along with rectangular and circular with equal width and height dimensions. These ribs are placed along the length of the channel equidistantly. Only one set of operating parameters considered and compared with the Baseline case parallel flow channel where no partial ribs is present. The study is conducted using the commercial software package ANSYS Fluent version 2023R2. The objective is to comprehend the effects of ribs on the polarization curve, i.e., current vs. voltage (I-V) curve as well as current vs. power (I-P) curve, pressure drop in the flow channels and oxygen consumption in fuel cell.

2. NUMERICAL MODEL DEVELOPMENT

2.1 Assumptions

Assumptions used in the present study includes:

- Flow of reactant gases is laminar and considered as ideal gas.
- Steady state condition.
- Two phase flow.
- Membrane, CLs and GDLs are considered as isotropic in nature.
- Heterogeneous electrochemical reactions occur at CL.

- Materials have constant values for thermal conductivities for average temperature.
- Contact resistance is considered between current collector and GDL.

2.2 CAD Geometry and Mesh

The present study involves three different parallel channels namely Fig. 1 :-

Baseline: Parallel channel with no ribs.

Concept 1: Parallel channel with rectangular ribs.

Concept 2: Parallel channel with circular ribs.

Concept 3: Parallel channel with airfoil ribs.

The Baseline has been referred from the works of Yuan et al. [1]. The details of the ribs' dimensions are listed in Table 1. Each of the ribs is placed equidistantly at 1mm. There are 15 ribs along the length of the flow channel. The geometries are prepared in ANSYS Spaceclaim, and for mesh, ANSYS Meshing is used. For airfoil coordinates, NACA 4424 is referred to in this study.

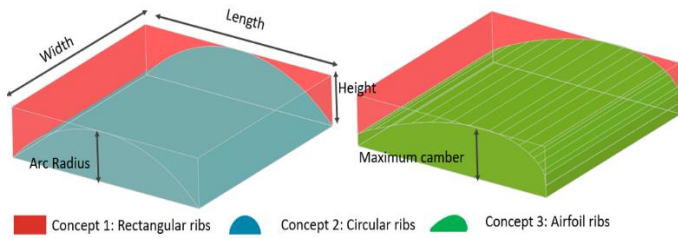


Fig. 1. Isometric view of different ribs

Hexahedral mesh is created for Baseline, Concept 1, Concept 2, and Concept 3. Same mesh strategy is employed for Baseline as per works of Yuan et al. [1]. Each of the Concepts is having 2472000, 2520000 and 2922980 cell count respectively.

Table 1: Dimensions of different ribs introduced in the parallel channel for present study.

Ribs	Length/ Arc Radius (mm)	Width (mm)	Height (mm)
Rectangular	1	1	0.2
Circular	0.725	1	0.2
Airfoil	1	1	0.2

2.3 Governing equations

Modelling of Electrochemistry

The movement of protons and electrons is primarily driven by the potential difference between the solid phase and the membrane phase or electrolyte. This potential difference is known as the local surface over-potential and is also referred to as activation loss. Two equations for solving potential: one for transport of electron through solid materials (conductive in nature) and the equations is solved at triple phase boundary of CL, solids of porous medium and current collector, and another for transfer of protons across membrane and this equation is solved at triple phase boundary of CL and membrane.

$$\nabla \cdot (\sigma_{sol} \nabla \phi_{sol}) + j_{sol} = 0 \quad (1)$$

$$\nabla \cdot (\sigma_{mem} \nabla \phi_{mem}) + j_{mem} = 0 \quad (2)$$

Where, j_{sol} and j_{mem} are the solid and membrane phase source terms. Also known as volumetric exchange current densities and usually computed from Butler-Volmer equation given below:

$$j_a = j_{a,ref} \left(\frac{C_{H_2}}{C_{H_2,ref}} \right)^{\gamma_a} \left[e^{\frac{\alpha_a F}{RT} \eta_a} - e^{-\frac{\alpha_a F}{RT} \eta_a} \right] \quad (3)$$

$$j_c = j_{c,ref} \left(\frac{C_{O_2}}{C_{O_2,ref}} \right)^{\gamma_c} \left[e^{\frac{\alpha_c F}{RT} \eta_c} - e^{-\frac{\alpha_c F}{RT} \eta_c} \right] \quad (4)$$

The Butler-Volmer is used to calculate the transfer currents in CLs.

At anode domain,

$$j_{sol} = -j_a < 0, j_{mem} = j_a > 0 \quad (5)$$

At cathode domain,

$$j_{sol} = j_c > 0, j_{mem} = -j_c < 0 \quad (6)$$

One can solve over-potential using

$$\eta = \phi_e - \phi_{mem} - V_{ref} \quad (7)$$

For anode domain,

$$V_{ref} = 0 \quad (8)$$

$$\eta = \phi_c - \phi_{mem} \quad (9)$$

For cathode domain,

$$V_{ref} = V_{OC} \quad (8)$$

$$\eta = \phi_c - \phi_{mem} - V_{OC} \quad (10)$$

Where V_{ref} and V_{OC} are reference electrode potential and open circuit voltage respectively. V_{OC} is computed from Nernst equation given as:

$$V_{OC} = E = -\frac{\Delta G_0}{2F} + \frac{RT}{2F} \ln \left[\frac{P_{H_2} P_{O_2}^{0.5}}{P_{H_2O}} \right] \quad (11)$$

Equation for Species Transport

The equation for species transport is defined with reference to Fick's Law as:

$$\frac{\partial(\varepsilon.c_k)}{\partial t} + \nabla \cdot (\varepsilon \vec{u} c_k) = \nabla \cdot (D_k^{eff} \nabla c_k) + S_k \quad (12)$$

Here, S_k is the source term for species and differs for each component of a PEMFC.

$$S_k = 0 \quad (13)$$

$$S_{H_2} = -\frac{1}{2FC_{total,a}} j_a \quad (14)$$

$$S_{O_2} = -\frac{1}{4FC_{total,c}} j_c \quad (15)$$

$$S_{H_2O} = \frac{1}{2FC_{total,c}} j_c \quad (16)$$

Eq. 13 is applied to membrane, GDLs and CLs. Whereas Eq. 14-16 are applicable for hydrogen, oxygen and water source terms at CLs.

D_k or gas diffusivity is computed at reference conditions of pressure and temperature (p_0, T_0) for species 'k' as follows

$$D_k = \varepsilon (1 - s)^{r_s} D_k^0 \left(\frac{p_0}{p}\right)^{\gamma_p} \left(\frac{T}{T_0}\right)^{\gamma_t} \quad (17)$$

Continuity equation

The continuity equation is described as under:

$$\frac{\partial(\varepsilon\rho)}{\partial t} + \nabla \cdot (\varepsilon\rho\vec{u}) = S_m \quad (18)$$

S_m is the source term for mass and equal to zero for entire fuel cell domain.

To model two-phase flow, the mixture density is established using the following forms of linear interpolation:

$$\rho = s_l \rho_l + s_g \rho_g \quad (19)$$

$$s_l + s_g = 1 \quad (20)$$

In this context, s represents volume fraction where l and g indicate liquid and gas phases, respectively.

Momentum equation

The equation for momentum is denoted as:

$$\frac{\partial(\varepsilon\rho\vec{u})}{\partial t} + \nabla \cdot (\varepsilon\rho\vec{u}\vec{u}) = -\varepsilon\nabla P + \nabla \cdot (\varepsilon\mu\nabla\vec{u}) + S_p \quad (21)$$

Here, S_p is the source term for momentum and equal to zero for flow channels.

Also, Darcy's law is used to express for porous material, as

$$\varepsilon\vec{u} = -\frac{k_p}{\mu} \nabla P \quad (22)$$

For gas and liquid mixture phases, μ is indicated by

$$\mu = s_l \mu_l + (1 - s_l) \mu_g \quad (23)$$

Thus, velocity is expressed as:

$$u = \frac{s_l \rho_l \mu_l + s_g \rho_g \mu_g}{s_l \rho_l + s_g \rho_g} \quad (24)$$

Energy equation

The comprehensive representation of the energy equation is:

$$\frac{\partial(\varepsilon.\rho.c_p T)}{\partial t} + \nabla \cdot (\varepsilon.\rho.c_p \vec{u} T) = \nabla \cdot (k^{eff} \nabla T) + S_Q \quad (25)$$

Where S_Q is the source term referred as given below

$$S_Q = I^2 R_{ohm} + \beta S_{H_2O} h_r + r_w h_l + \eta R_{a,c} \quad (26)$$

Each term refers to ohmic heating, heat of formation of water, electric work and latent heat respectively [1].

Liquid water generation and its transport

For modelling the liquid water formation and its transport, the reader is advised to refer the work of Yuan et al. [1] and ANSYS Fluent User Manual [13].

2.4 Boundary conditions

- Mass flow inlet at inlets of each channel.
- Pressure outlet at outlets of each channel.
- Wall are assigned stationary.
- A zero-flux boundary condition is imposed on the membrane phase potential at all outer boundaries because no protonic current escapes through any external boundary of the fuel cell, ensuring $\frac{\partial \phi_{mem}}{\partial n} = 0$.
- The solid phase potentials on the external contact boundaries are established as fixed values, acting as potential static boundary conditions. For this model, the solid phase potential on the anode side is set to zero $\phi_{s,anode} = 0$. While on the cathode side, it matches the cell voltage, $\phi_{s,cathode} = V_{cell}$.

The operating conditions and physical specifications are listed in Table 2 and materials in Table 3. Values of reference exchange current density, concentration exponent, exchange coefficient, reference diffusivity, porosity, contact angle, absolute permeability, surface-to-volume ratio, membrane properties like equivalent weight, protonic conduction coefficient and exponent are sourced from Yuan et al. [1].

Table 2: Material specifications of different components of PEMFC.

Parameters/Components	Membrane	CL	GDL	Current collector
Density (kg/ m ³)	1980	2010	490	1880
Specific heat (J/kg K)	2000	710	710	875
Thermal conductivity (W/m K)	0.67	8	1.6	10.7
Electrical conductivity (S/m)	1.23	1000	5000	83000

Table 3: Operating conditions and physical specifications of different components of PEMFC

Operating temperature (°C)	80
Operating pressure (Pa)	200000
Pressure at channel outlet (Pa)	0
Relative humidity at anode and cathode (%)	100
Stoichiometry (hydrogen/oxygen)	1.5/ 2
Contact resistance between CL and GDL	2e-06

3. RESULTS AND DISCUSSION

The present study investigates the performance of PEMFC through polarization curves including the current vs. voltage (I–V) curves and current vs. power (I–P) curves. Here, in this paper, one set of operating conditions is utilized.

3.1 Model validation with experimental results

Fig. 2 represents the comparative data on performance for Baseline PEMFC model through the current vs. voltage (I–V) curve between the published experimental and numerical results of Yuan et al. [1] and present numerical study. Minor difference with an average error band of less than 5% ranging from (200 to 1200 mA/cm²) and (0.73 to 0.38 V) is observed between the published experimental and present numerical results. Thus, confirming the present numerical model. Indicating it is proficient in predicting the effects of variable operating parameters on the performance of PEMFC.

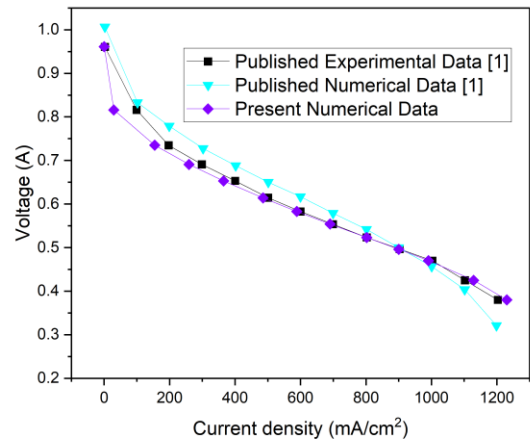
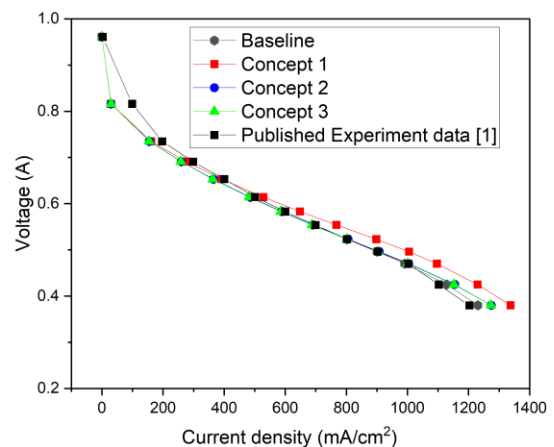


Fig. 2. Numerical validation of Baseline with published work of Yuan et al. [1] for I-V curve.

3.2 Effect of ribs in the performance of PEMFC

Fig. 3 represents the polarization curves, i.e., the current vs. voltage (I–V) curves and current vs. power (I–P) for all three Concept designs of parallel flow channel with different ribs configurations. Concept 1 is predicting higher performance when compared with Baseline (present numerical result as well as published experimental result), Concepts 2 and 3. Whereas, Concepts 2 and 3 are having similar polarization curves still higher than Baseline. At low current density the Concepts 1, 2 and 3 predict similar trend for high voltages. Beyond 0.65 mA/cm² Concept 1 predicts higher voltages when compared to Concepts 2 and 3 respectively. Similar, trend is observed for I–P curves as well (Fig. 4).

Fig. 3. I-V curves of different parallel flow channel designs compared with published experiment data [1]



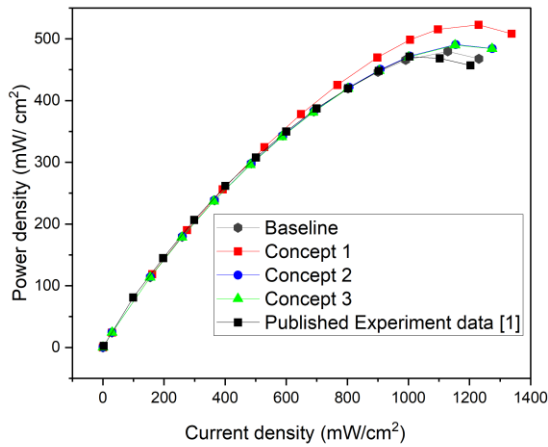


Fig. 4. I-P curves of different parallel flow channel designs compared with published experiment data [1]

It is observed that ribs in channel aid in delivery enhancement of reactant gases to the CLs sites of reaction, hence improving the overall performance of PEMFC. At the start of operation in a PEMFC, the rate of consumption of reactant gases is low. In low current density region although the activation loss is high, but the concentration loss is low. Hence, a drop is observed initially low current density and high voltage region of the polarization curves. In the present study, at an operating temperature and pressure of 80°C and 2 MPa respectively, from Fig.4, it is observed that Concept 1 delivers the highest power density of 522.62 mW/cm². Correspondingly, Baseline, Concepts 2 and 3 records 479.7, 490.7 and 489.7 mW/cm².

3.3 Enhancement in pressure drop

Figs. 5 and 6 represents the pressure drop curves for all designs for each of the flow channels- anode and cathode. High pressure drop is observed for Concept 1, followed by Concept 3. Minimal difference is recorded for Concept 2 and 3. All three Concept designs have higher pressure drops compared to Baseline.

3.4 Enhancement in oxygen consumption

The idea of using indentation in channels in the form of ribs is to enhance the mass transport, thereby reducing the loss due to concentration. In a scenario where there is low current density and high voltage, the effect of concentration losses is minimal, making channel indentation ineffective in regions of low current density. Here, the oxygen consumption rate is low, providing ample time for oxygen to reach the catalyst layer (CL) reaction sites. Therefore, using ribs to guide oxygen to the CL isn't necessary, and channel ribs doesn't

significantly improve the cell performance. In contrast, in areas of high current density, the oxygen consumption rate is high, which may cause oxygen shortages at reaction sites. Thus, channel ribs can enhance oxygen delivery to these sites to mitigate this effect.

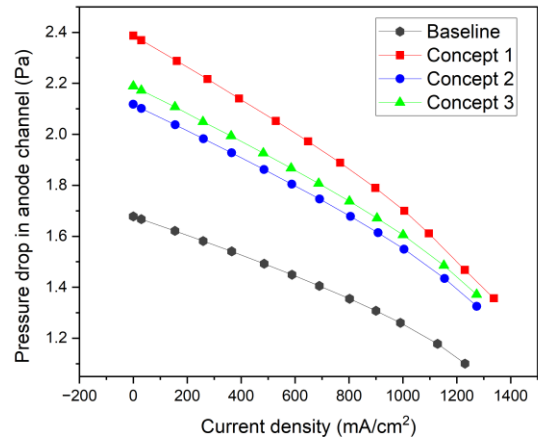


Fig. 5. Pressure drop vs. current density curves of different anode parallel flow channel designs.

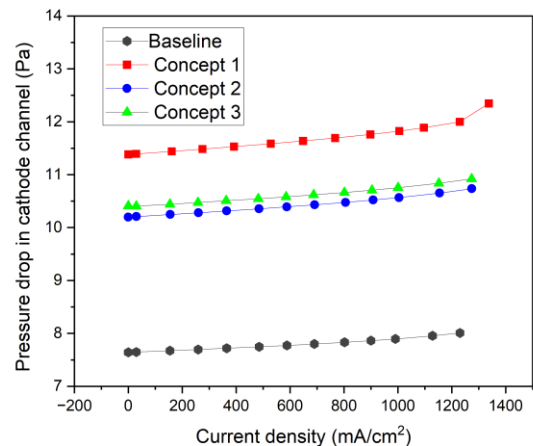


Fig. 6. Pressure drop vs. current density curves of different cathode parallel flow channel designs.

Fig. 7 indicates that the mole fraction of oxygen diminishes along the channel due to consumption. High rate of oxygen consumption at the interface of CL and GDL in the cathode domain for Concept 2 and 3 compared to Baseline is visualized here.

4. CONCLUSIONS

The parallel flow channels with partial ribs predict high performance than parallel flow channels with no ribs. High performance is predicted through the polarization curves, i.e., the current vs. voltage (I-V) curves and

current vs. power (I-P) for Concept 1 amongst the designs.

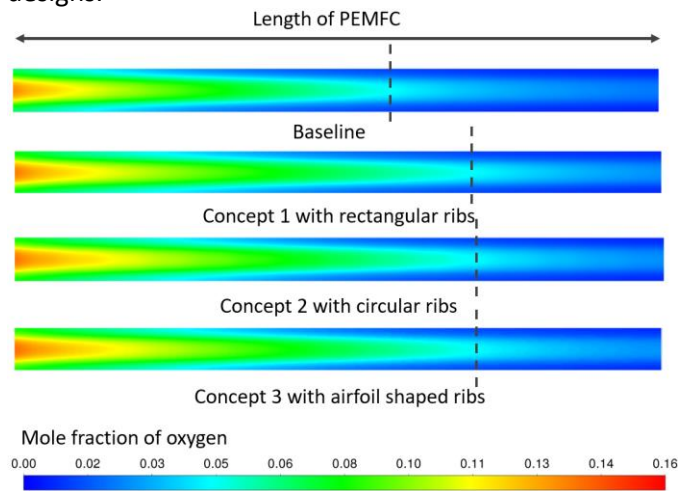


Fig. 7. Mole fraction of oxygen or rate of oxygen consumed at the interface of cathode CL and GDL.

However, Concepts 2 and 3 predicts similar polarization curves. At low current density the Concepts 1, 2 and 3 predict similar trend for high voltages. Beyond 0.65 mA/cm^2 Concept 1 predicts higher voltages when compared to Concepts 2 and 3 respectively. From power density perspective, Concept 1 delivers the highest power density of 522.62 mW/cm^2 . While Baseline, Concepts 2 and 3 records 479.7 , 490.7 and 489.7 mW/cm^2 . However, despite predicting higher performance, Concept 1 has the highest pressure-drop in comparison to existing designs, followed by Concept 3. Ribs are responsible for reduction in the cross-sectional area of the flow channel, leading to flow restriction and increase in pressure. It is also observed that mole fraction of oxygen diminishes along the channel due to consumption. High rate of oxygen consumption at the interface of CL and GDL in the cathode domain for Concept 2 and 3 when compared to Baseline. From practicality perspective, Concept 1 is easier to manufacture compared to other concepts (especially Concept 3 with airfoil shape) but with a trade-off on pressure drop.

ACKNOWLEDGEMENT

Cummins Technologies India Pvt. Ltd. for allowing the use of computational resource for the present study.

REFERENCE

[1] Yuan W, Tang Y, Pan M, Li Z, Tang B. Model prediction of effects of operating parameters on proton exchange membrane fuel cell performance. *Renewable Energy* 2010; 35:656–666.

[2] Tiss F, Chouikh R, Guizani A. A numerical investigation of reactant transport in a PEM fuel cell with partially blocked gas channels. *Energy Conversion and Management* 2014;80:32–38.

[3] Li X, Sabir I. Review of bipolar plates in PEM fuel cells: flow field designs. *Int J Hydrogen Energy* 2005;30:359-71.

[4] Scholta J, Escher G, Zhang W, Kuppers L, Jorissen L, Lehnert W. Investigation on the influence of channel geometries on PEMFC performance. *J Power Sources* 2006;155:66-71.

[5] Wang XD, Duan YY, Yan WM, Peng XF. Effects of flow channel geometry on cell performance for PEM fuel cells with parallel and interdigitated flow fields. *Electrochim Acta* 2008;53:5334-43

[6] Sun L, Oosthuizen PH, McAuley KB. A numerical study of channel-to-channel flow cross-over through the gas diffusion layer in a PEM-fuel-cell flow system using a serpentine channel with a trapezoidal cross-sectional shape. *Int J Therm Sci* 2006;45:1021-26.

[7] Ahmed DH, Sung HJ. Effects of channel geometrical configuration and shoulder width on PEMFC performance at high current density. *J Power Sources* 2006;162:327-39.

[8] Ghanbarian A, Kermani MJ. Enhancement of PEM fuel cell performance by flow channel indentation. *Energy Conversion and Management* 2016;110:356–366

[9] Wang XD, Huang YX, Cheng CH, Jang JY, Lee DJ, Yan WM, et al. An inverse geometry design problem for optimization of single serpentine flow field of PEM fuel cell. *Int J Hydrogen Energy* 2010;35:4247-57.

[10] Heidary H, Kermani MJ. Enhancement of heat exchange in a wavy channel linked to a porous domain; a possible duct geometry for fuel cells. *Int J Heat Mass Transfer* 2012;39:112–20.

[11] Shimpalee S, Van Zee JW. Numerical studies on rib & channel dimension of flow-field on PEMFC performance. *Int J Hydrogen Energy* 2007;32:842-56.

[12] Hsieh SS, Chu KM. Channel and rib geometric scale effects of flow field plates on the performance and transient thermal behavior of a micro-PEM fuel cell. *J Power Sources* 2007;173:222-32.

[13] ANSYS® Fluent, 2023 R2, Ansys Fluent Users Guide, ANSYS, Inc.